H. R. Rottmann

Overlay in Lithography

Advances in lithography rely largely on the capability of reducing overlay errors, which in turn depends on the capability to make two-dimensional overlay measurements. This paper describes a simple and accurate method of determining singular overlay errors of step-and-repeat exposure systems with a precision of $\pm 0.01~\mu m$ (standard deviation).

Introduction

Fabrication of integrated circuits (ICs) requires that pattern arrays which delineate individual layers of integrated circuits must meet satisfactory registration tolerances. Advances in IC fabrication depend primarily on the capability of reducing these tolerances, which are determined by the variation of critical pattern locations and sizes. Present pattern sizes can be as small as $2-3 \mu m$ and further reductions can be expected. The corresponding registration or overlay tolerances between superimposed patterns on the wafer must only be a fraction of this value. Furthermore, this fraction must be subdivided to accommodate the wafer-to-mask alignment and other overlay errors introduced by equipment, material, and environmental factors. Consequently, a reduction of these overlay errors should play a decisive role in future lithographic developments.

The objective of this paper is to determine individual mask-overlay errors because masks present the first and most critical step of IC fabrication, and mask dimensions (and errors) are more difficult to measure than those for wafers. At present, measurement machines [1-4] are used to determine the total overlay error of masks. Errors between different masks are determined by subtracting corresponding long-distance measurements. Inevitably, the uncertainty of $0.1-0.2~\mu m$, introduced by the measurement process and by system bias of $0.2-0.4~\mu m$, makes accurate performance evaluations and improvement of lithographic equipment difficult if not impossible. This paper presents a method to overcome this problem by use of overlay; the uncertainty of measurement is better than $0.03~\mu m$ (3σ).

Mask registration

Misregistration between masks of a set is introduced by $10\times$ pattern generators, $10\times$ reticle alignment, and $1\times$ step-and-repeat exposure (also called *stepping*). The first two systems are relatively easy to evaluate because they either operate at $10\times$ or are well understood from a theoretical viewpoint. The stepping machine, on the other hand, is more difficult to analyze because it is by design a complex system and its total overlay error is small to begin with ($\approx 0.5~\mu$ m). In this paper we address primarily registration errors introduced by stepping systems.

The stepping machine is a reduction camera that generally reduces a reticle mask by a factor of ten; the size of the $1 \times$ field can exceed 10 mm \times 10 mm. The $1 \times$ mask is supported on x-y stepping tables that make successive exposures of fields (chips) possible over areas of up to 150 mm on the side. Detailed descriptions of step-and-repeat cameras have been published and are also available from vendors [5-8].

The basic requirement of such a system is to produce two-dimensional arrays of patterns with a minimal amount of unpredictable and uncontrollable disorder. Three types of variables can be expected to influence pattern locations. First, the array of stepped patterns depends on interferometrically controlled table positioning. Typical errors are non-straightness of travel, deviation from orthogonality of the x and y axes, and lack of repeatability of stepping. Second, the state of the resist-coated substrate adds uncertainty in terms of uncontrollable topographic deformations due to clamping and temperature

Copyright 1980 by International Business Machines Corporation. Copying is permitted without payment of royalty provided that (1) each reproduction is done without alteration and (2) the *Journal* reference and IBM copyright notice are included on the first page. The title and abstract may be used without further permission in computer-based and other information-service systems. Permission to *republish* other excerpts should be obtained from the Editor.

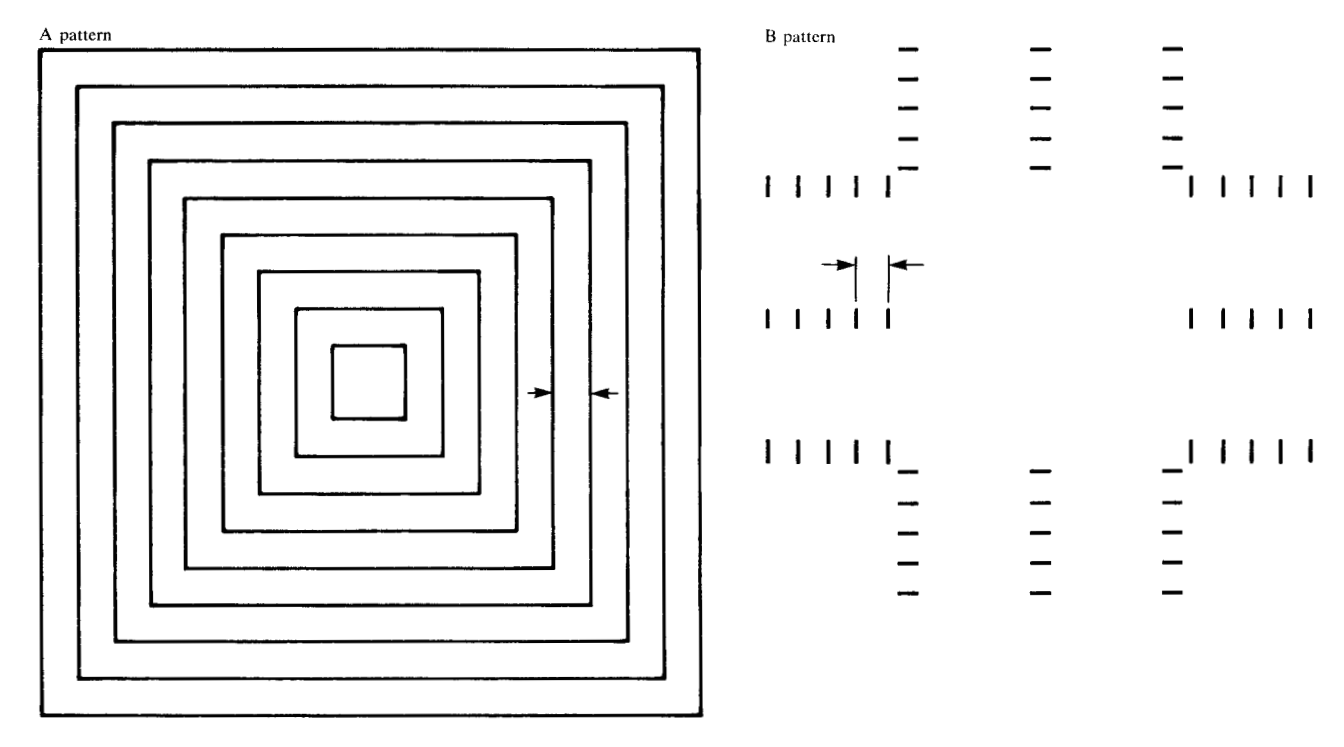


Figure 1 Special two-dimensional patterns for measurement of overlay errors. Patterns A and B have slightly different periodicities (25 μ m for A, 22.5 μ m for B, as measured from line center to line center) to ensure suitable measurement conditions despite mask-placement variations.

changes. Third, changes of pattern locations can occur within a stepped field because of asymmetric irradiance distributions in the image plane. The size of some of these errors can be expected to be $<0.1~\mu m$ and therefore presents a challenge to the design engineer.

A solution to the problem of accurate overlay measurement is provided by application of special patterns and measurement with automatic linewidth (i.e., short-distance) measurement microscopes. This approach permits determination and analysis of individual stepping errors in both axes for both short- and long-term performance studies.

Method of measurement

The most accurate method of measuring step-and-repeat exposure system performances is provided by the photolithographic process itself. This process permits addition of patterns to an array of primary or reference patterns generated either by another system or by the same system at an earlier point in time. Figure 1 shows primary and secondary types of line patterns that have proved effective. The patterns, denoted as A and B, are two-dimensional and the dark lines (transparent areas) are $\approx 2.5 \ \mu \text{m}$ wide. The chrome spaces between the lines are, respectively, 25 and 22.5 μm wide for A and B patterns.

The slightly different periodicity of the sets of primary and secondary lines is important if the mask has been moved between array exposures, e.g., to measure longterm drift, or if it has been placed on a second system to determine differential overlay. Regardless of the mask placement errors, at least one of the secondary (measurement) lines lies in the space between two adjacent reference lines without coming too close ($\geq 1 \mu m$). Figure 2 shows two extreme cases of superimposed A and B patterns. The B patterns are usually added at a later date (perhaps many months later) by use of the same or another lithographic system. The degree of registration or overlay between the two layers at each exposure step can now be determined with an automatic linewidth-measuring microscope. The objective of measurement is to determine any unexpected and nonuniform errors between related A and B patterns of the stepped fields.

Generally, there are four modes of pattern application. First, the A patterns alone are exposed by step-and-repeat (stepped). They are placed close to each other so that the space between adjacent peripheral lines is within the range of measurement. This permits not only determination of stepping errors between adjacent cells in both axes, but also measurement of cell-size variations because of uncertainty of focus. Second, immediately after

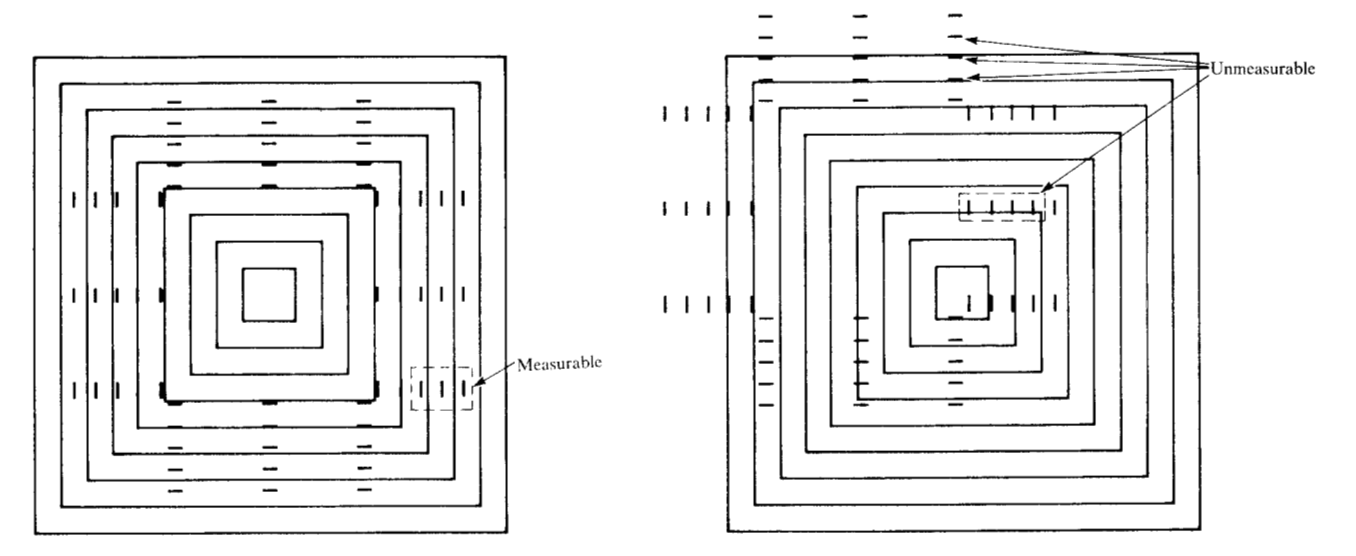


Figure 2 Two extreme cases of superimposed A and B patterns with examples for measurable and unmeasurable lines.

stepping a $1\times$ array of A patterns, the same sequence is repeated with the B patterns, only the $10\times$ A pattern is replaced by the $10\times$ B pattern between the two exposure runs. The $1\times$ substrate remains rigidly clamped during successive stepping runs. This provides determination of short-term stepping errors. Third, after the A array is completed, the substrate is removed and the B patterns are exposed either on a second system or on the same system at a later point in time in order to assess, e.g., long-term system behavior. In this case, the initial location of the substrate is lost after the A array is stepped because the substrate is removed and small Δx , Δy , and $\Delta \theta$ placement errors occur when the substrate is returned for the second, third, etc., exposure sequence.

In the three preceding cases the orientation of the substrate remained unchanged between the A and B exposure sequences. In the fourth mode of application, the substrate is rotated either by 90° or 180° between the stepping of the A and B patterns to determine asymmetries in the two-dimensional stepping system. The general objective in all cases is to determine changes from uniformity. The individual measurement objective is always determination of the spaces between line centers.

Measurement accuracy is expected to be <0.03 μ m, especially if differential measurements are performed [9]. This can be achieved by determination of the distance D between the center of the interval A (distance between A pattern lines) and the center of line B [see Fig. 3(a)]: D = (L - R)/2, where L and R are defined in Fig. 3(a). The variations in D for each step represent errors between

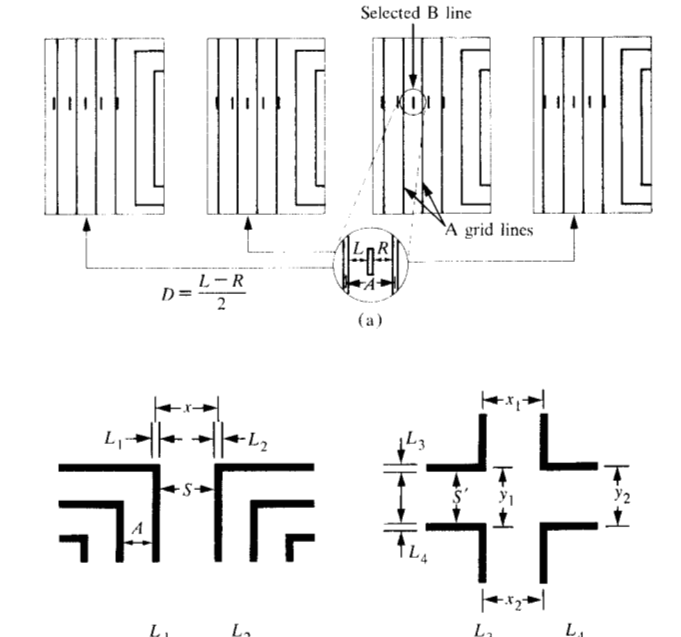


Figure 3 (a) Portions of four step-and-repeat exposed A and B patterns. For each step, the same B line is used for measurement relative to the A grid lines. (b) The A patterns have been stepped in close proximity to measure the interval x. (c) As in (b) but measurement of interval y.

successively stepped arrays. An accurate calibration of the measurement microscope is unnecessary if $L \approx R$. This condition is met inherently because of the multiplic-

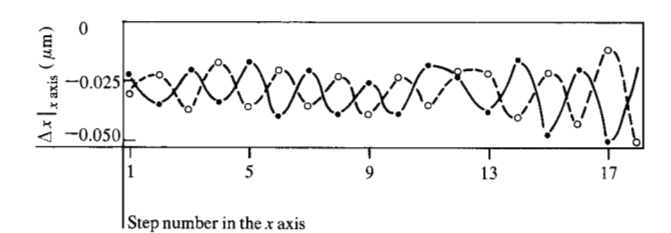


Figure 4 The variations of $\Delta x|_{x \text{ axis}}$ plotted for two adjacent rows in the x axis.

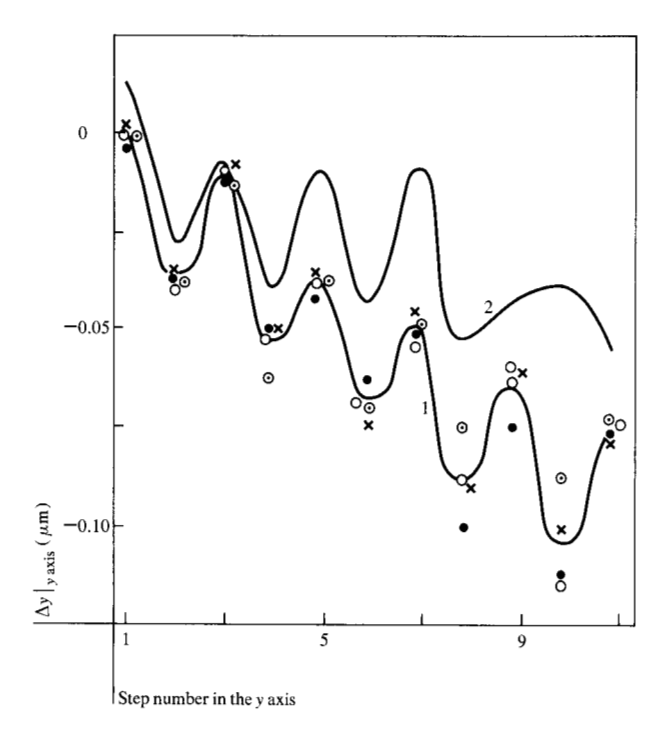


Figure 5 The variations in $\Delta y|_{y \text{ axis}}$ for two different masks. The systematic errors were caused by system hysteresis and misalignment of the interferometer. The curves show averages of four stepped columns. Individual data points for the four columns are shown in Curve 1 only.

ity and the slightly different periodicities of the A and B target lines; it also facilitates measurement with an automatic linewidth-measurement microscope since the size and the separation of the two gate rectangles on the video screen do not have to be readjusted from site to site. Errors introduced by placement (if the plate was removed) are of no concern since they represent only an $x-y-\theta$ transformation of the entire array and therefore can easily be removed.

Experimental results

The total registration error between a set of masks is determined by a variety of sources affecting the relative locations of the stepped patterns. Ideally, the stepped patterns should be equally spaced so that associated images of any two overlaid masks would display perfect registration. In practice, however, the stepped images are affected by various random and systematic errors that depend on design and performance characteristics and on adjustment of the stepping system.

• Stepping errors

Two modes of measurement have been studied: that between adjacent steps of the same stepping sequence (A patterns only) and that between identical steps of subsequently stepped arrays (B patterns superimposed on A patterns).

The periodicity of stepping the A pattern was selected such that the peripheral lines of adjacent steps were sufficiently close to each other. After completion, the first $10\times$ segment was replaced by the B pattern, the stepping table was returned to the origin, and the same sequential array was stepped with the second pattern either immediately or after several days or weeks. If desirable, this operation can be repeated several times provided only one of the identical target sets is used for each sequence while the others are masked off.

Figure 3(a) shows sections of overlaid patterns for determination of stepping errors in the direction of the x axis (abbreviated $\Delta x|_{x \text{ axis}}$). Note that the selected lines of the A and B patterns in this case are parallel to the y axis. The same definition can be applied to stepping errors in the direction of the y axis ($\Delta y|_{y \text{ axis}}$), where A and B lines are parallel to the x axis. Finally, straightness of travel in both axes is denoted as $\Delta y|_{x \text{ axis}}$ and $\Delta x|_{y \text{ axis}}$. In both cases the A and B lines, which represent the measurement targets, are parallel to the corresponding axis of stepping.

The first objective is measurement of the intervals x = $(L_1/2) + S + (L_2/2)$ [as shown in Fig. 3(b)] and $y = (L_2/2)$ + S' + $(L_4/2)$ [Fig. 3(c)], where the L_n are linewidths. These numbers represent the relative distances between two adjacent cells in the x or y axis. Figure 4 shows values of x for two rows that were stepped in opposite directions; Fig. 5 shows individual and averaged values of y for four rows on two plates. The curve for plate 2 shows only the average. The range in the x and y directions was ≈75 mm. Both examples demonstrate the performance of the interferometric feedback system of the stepping machine. The corrective actions are remarkably periodic. switching between states of advance and delay and being out of phase for the two rows that were stepped in opposite directions; see Fig. 4. This case represents stepping errors Δx in the x axis $(\Delta x|_{x \text{ axis}})$. Stepping errors in the y axis $(\Delta y|_{y \text{ axis}})$ are similar, but remain in phase, because

the advance is unidirectional; see Fig. 5. Misalignment of the y laser beam adds a ramp to the oscillatory curve. The oscillations can be explained in terms of the opposite directions of stepping in the x axis, which causes a small amount of hysteresis parallel to the y axis. Further experimental detail can be found in Ref. [9].

Figure 6 shows measurement of the differential straightness of travel $(\Delta y|_{x \text{ axis}})$ for adjacent rows of stepping in the x direction and measurements similar to those of Fig. 3(c). The interferometrically controlled feedback system kept the random variations well within $\pm 0.02~\mu\text{m}$; however a small systematic shift in the y axis ($\approx 0.03~\mu\text{m}$) may occur as with mask no. 3 (top two curves in Fig. 6). Other measurements have been performed, such as differential straightness of travel between the x and y axes. For this purpose, the mask was rotated by 90° after exposure of the A array and the B array was then exposed. Variations up to $\pm 0.10~\mu\text{m}$ can be explained primarily in terms of the tolerances of the interferometer mirrors.

• Table orthogonality

Determination of orthogonality between the two superimposed stepping tables provides an example for performing absolute measurements. For this purpose, a row and a column of pattern A are step-and-repeat exposed through the center of the mask with the individual patterns being closely spaced; see Fig. 7(a). The patterns display a "cross" that bisects the mask in both directions; note that $\theta_A = \theta_B$. After completion, the $10 \times A$ pattern is replaced by the B pattern, the $1 \times$ plate is rotated by 90° and secured, and a second cross is stepped over the first one. For simplicity, we now rotate the axes such that the horizontal A and B axes (x axes) are parallel [see Fig. 7(b)] and measure 2θ .

After processing, the position of the B cross is determined against that of the A cross at seven locations by using measurable A and B lines (see column 1 of Table 1). The second column shows the relative differences in Δx and Δy at the sampling sites (zero would indicate orthogonality). The orthogonality was determined for each individual case, as shown in the third column. From these values one can calculate the deviation of the table orthogonality; the individual variations are a measure of the interferometer mirror quality, stepping errors, and measurement errors. Addition of more points of measurement further increases the accuracy of the orthogonality measurement because the degrading influence of the other factors is diminished.

• Substrate deformation due to mechanical stress Substrates generally are vacuum clamped on the backside to avoid any irregular motion during step-and-repeat ex-

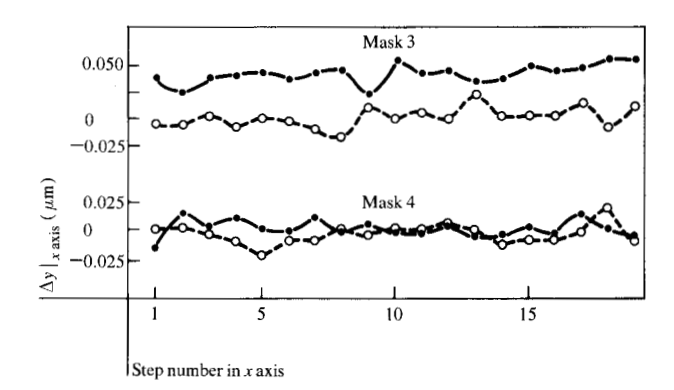


Figure 6 Differences of straightness of travel $(\Delta y|_{x \text{ axis}})$ between adjacent rows $(1, 2, \bullet; 2, 3, \bigcirc)$ using closely spaced A patterns for two different masks.

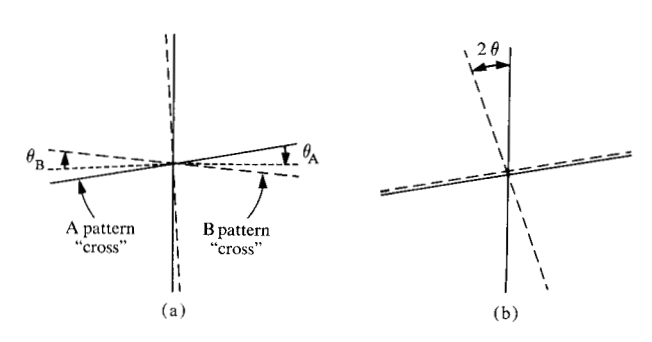


Figure 7 Measurement of the deviation from orthogonality by rotation of the mask by 90° (see text).

Table 1 Determination of deviations from orthogonality.

Relative position on mask (mm)	$\frac{ \Delta x - \Delta y }{(\mu m)}$	2θ (arc-s)
10	≈0	≈0
20	0.075	0.80
30	0.210	1.40*
40	0.270	1.34*
50	0.390	1.54*
60	0.530	1.74*
70	0.510	1.42*

^{*}The average of these values is $\approx 1.5 \pm 0.2$ arc-s.

posures [10]. However, excessive clamping forces can distort the surface of the mask unless special precautions are taken to ensure deflection-free clamping [9]. Such mask-surface deformations due to improper clamping vary from mask to mask in an unpredictable fashion because of backside surface variations. The following procedure is uniquely suited to determine the distortion of

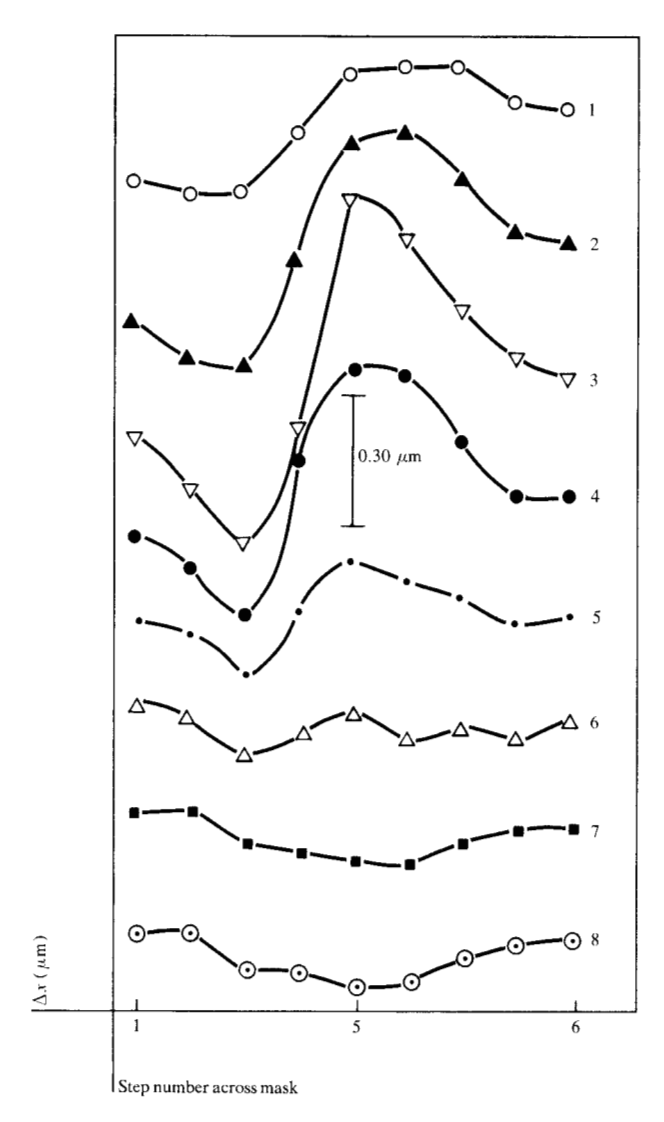


Figure 8 Influence of mask deformation on overlay. The deviation from horizontal lines (the ideal case) is caused primarily by the differences of overlay Δx due to the change from a clamped-to a free-state mask support. The numbered curves refer to row numbers.

overlay due to surface deformations. A substrate is placed onto the stepping table and vacuum clamped, and an array of A patterns is exposed. Subsequently, the vacuum clamping system is deactivated and the substrate is returned to its natural stress-free state. To avoid any motion during stepping the substrate is secured by means of small pieces of wax along its sides without disturbing its relaxed state. Now the B patterns are exposed. After development and etching of the chromium film, the relative positions of the A and B patterns were measured, as discussed earlier. The results, shown in Fig. 8, clearly dis-

play the impact of surface deformations on mask overlay. The errors vary from mask to mask because of differing mask backside topographies, nonrepeatability of clamping due to statistical effects related to friction, and minute particles (burrs) between the mask and clamping surfaces. These nonlinear errors range from ≈ 0.1 –0.4 μ m, and therefore can exceed the stepping error by a factor of ten. It is estimated that generally between 5 and 20% of the chips are affected.

• Substrate deformation due to temperature

Overlay errors introduced by temperature differences of the masks can be studied in a similar fashion, as demonstrated in Fig. 9(a). First an array of A patterns is stepped. Then rows 1 and 10 are exposed with pattern B, keeping all other factors constant. These two rows establish the reference data. Subsequently, the upper right corner and lower center region of the mask are heated by touching (operator's finger) for ≈ 25 s. Thereafter, stepping of rows 2 through 9 is completed with pattern B. Figure 9(b) shows the resulting overlay distortion. (The stepping range was 60 mm.)

• Change of field size

The preceding examples discussed the registration errors of stepping systems under the assumption of small diffraction-limited fields. Fabrication of LSI circuits, however, requires replication of 2-3- μ m lines over field sizes approaching and perhaps even exceeding 10 mm \times 10 mm. This raises the question of potential changes of registration within the fields or between fields [10].

In order to assess this contribution under manufacturing conditions, a monitoring effort was initiated. The same 10× reticle containing A patterns in the four corner regions of the field was stepped once per week over an extended period of time. A periodicity of 8.5 mm was selected; it placed the outermost lines of the 1× fields close enough to permit measurement of the space between adjacent fields with the automatic linewidth-measuring microscope. Four measurements [shown in Fig. 3(c)] were made: x_1 , x_2 , y_1 , and y_2 . These provide a measure of the field size. A total of ten fields per mask were measured in this fashion and the average \bar{x}_1 , \bar{x}_2 , \bar{y}_1 , and \bar{y}_2 values were calculated in order to further reduce the small stepping errors (e.g., as shown in Fig. 4). The results for two systems over a period of about 55 days are plotted in Figs. 10(a) and (b). Ideally, these curves should all coincide and be horizontal. The actual results demonstrate that the $1\times$ size of a square field generally varies even with the same 10× input, that parallel sides can vary by different amounts, that variations from $\approx 0.04-0.40 \mu m$ have been detected, and that systematic errors between both systems are clearly discernible.

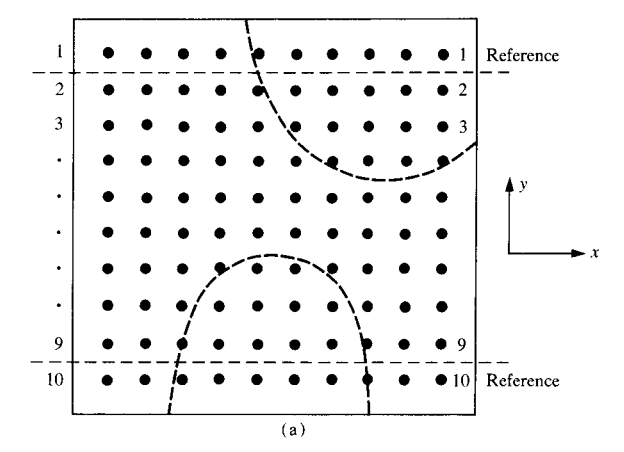
The preceding measurements were performed on equipment that is in continuous use for production of $1\times$ masks and is therefore not available for precise analysis of the causes of these changes. The following mechanism most likely is responsible. The spatial-intensity distributions in the imaginary-image plane display varying degrees of asymmetry because of aberrations and assemblage errors. The photoresist film on the substrate intersects the image plane in a not completely predictable fashion because of minute focusing errors. As a consequence, the edges of the images vary asymmetrically relative to their centers, causing slight displacements between images for which differences in these conditions prevail. Similar variations have also been observed with wafer exposure systems. This hypothesis was tested by deliberately changing the focal setting. A vertical change of the image plane by about 2 μ m resulted in a change of field size by about 0.12 μ m, despite the telecentric nature of the lens.

Measurement accuracy

Self-measurement of lithographic systems, as demonstrated in this paper, provides four important advantages over conventional long-distance measurement systems. First, the overlay measurement accuracy is substantially improved because environmental fluctuations, measurement-equipment tolerances, uncertainty, and biases are either absent or negligible. Second, one can conduct special studies (e.g., on the influences of mask deformation, equipment drift, and temperature effects) that are difficult if not impossible to perform otherwise. Third, cost and energy consumption of the optical measurement apparatus are relatively small in comparison to large-scale measuring machines and environmental chambers. Fourth, the size of the substrate is not limited by the measurement system. One disadvantage, however, is that individual long-distance measurements cannot be performed.

The measurement uncertainty of the overlay method depends on the performance of the measurement microscope, vibration, and materials- and processing-related factors. We found the automatic linewidth-measuring microscopes that use video signals for measurement of image sizes to be uniquely suitable for this program. Their performance is determined by the degree of scatter of repeated edge-to-edge measurements. We have made such measurements and have obtained accuracies of $\pm 0.04~\mu m$ with a precision (standard deviation) of 0.01 μm [11, 12]. Thus, the technique appears quite feasible. The major source of error was attributable to minute vibrations of the microscope stage.

Many measurements in this paper represent differential readings such as D = (L - R)/2; see Fig. 3(a). This fact,



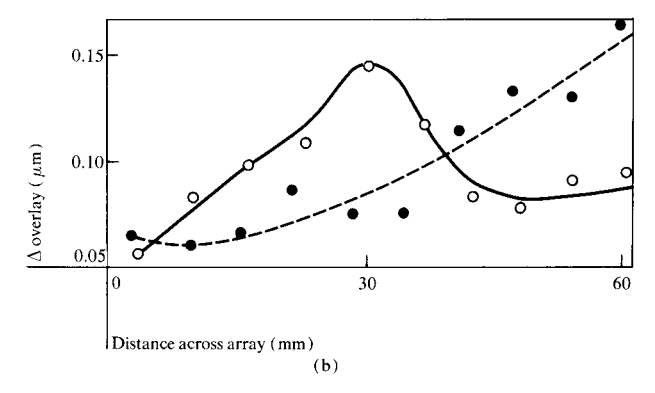


Figure 9 Impact of temperature on overlay. (a) The dots represent the A pattern array. Two regions were heated by touching (finger) for 25 s. The B pattern was then applied over the A array. (b) The differences in overlay between selected A and B lines for rows 2-4 (\bullet) and 7-9 (\bigcirc). Control rows 1 and 10 were "horizontal" within $\pm 0.03~\mu m$.

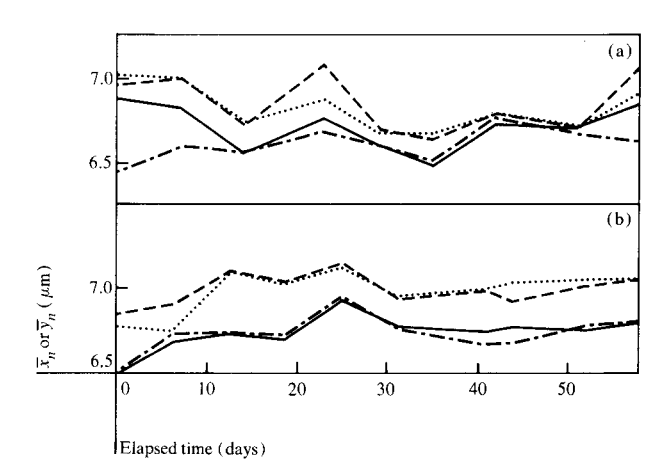


Figure 10 Values of \tilde{x}_1 (—), \tilde{x}_2 (——), \tilde{y}_1 (· · ·), and \tilde{y}_2 (——) for two stepping systems over a period of about 55 production days, using the same $10 \times A$ pattern.

in combination with a high degree of linearity of the measuring system, led us to conclude that the impact of small calibration errors on overlay measurements is insignificant. Selection of targets such that $D\approx 0$ (i.e., $L\approx R$) and division by the factor two provide further reductions in measurement uncertainty.

Two cases are of special interest. First, a mask with 100 (A νs . B) sites was measured and the same measurement sequence was repeated after nine months. The average difference between the two sets of numerals was 0.008 μ m; the standard deviation per measurement was 0.01 μ m. Second, we measured different target sets separated by up to 1 mm but associated with the same exposure step. These results indicate that the impact of spatial and process-related factors (e.g., ripple in the resist surface) on the measurement results can be kept smaller than $\pm 0.02~\mu$ m. If necessary, further improvements are feasible, e.g., by performing many repetitive sets of measurements to reduce the random measuring errors and errors introduced by minute dust particles or similar disturbances.

Many advantages accrue from this type of "self-measurement" in two axes. The overlay capabilities of lithographic systems can be determined with an accuracy which appears to exceed that of any other reported system. No Abbe errors occur since the reference and measurement arrays practically coincide. Environmental drift and fluctuations during measurements are negligible. This in turn permits determination of all kinds of singular causes of overlay degradation, some of which are difficult if not impossible to measure by other means. In addition, system performances can be monitored periodically to ensure the steady production of high-quality masks.

Summary

A major limiting factor in lithography is overlay distortion between different layers of patterns. A method for overlay measurement has been designed and implemented. It consists of a commercially available automatic linewidthmeasuring microscope and a set of special test patterns. Modes of application to make both absolute and relative measurements have also been described. Individual overlay errors were determined and it was found that the major errors are systematic or predictable; these range from ≈ 0.03 -0.40 μ m. The random errors are generally < 0.07 μ m. Application of this inexpensive and versatile method, e.g., to product-mask inspection or the analysis and improvement of other lithographic exposure systems, appears promising.

Acknowledgments

Numerous people at IBM's East Fishkill mask facility supported this project. Special thanks are due to L. Bureau, R. Lowry, J. McHugh, J. G. Simmons, and J. G. Williams.

References and notes

- F. R. Ashley, E. B. Murphy, and H. J. Savard, "A Computer Controlled Coordinate Measuring Machine," Bell Syst. Tech. J. 49, 2193 (1970).
- M. Alston-Garnjost, J. W. Davis, P. M. Daubner, and R. A. Smits, "A Large Granite Stage and Measuring Microscope," Rev. Sci. Instrum. 42, 1565 (1971).
- P. H. Coffee, "An X-Y Measurement System for Chrome Masks," Circuits Manufacturing 19, 98 (1979).
- Nikon measuring machine, Nippon Kogaku (USA) Inc., 623 Stewart Ave., Garden City, NY 11530.
- 5. F. T. Klostermann, "Step and Repeat Camera," *Philips Tech. Rev.* 30, 64 (1969).
- D. S. Alles, "The Step-and-Repeat Camera," Bell Syst. Tech. J. 49, 2145 (1970).
- Electromask (Subsidiary of TRE Corp.), 6109 DeSoto Ave., Woodland Hills, CA 91367.
- Mann Model 3696 photorepeater, GCA Corp., 174 Middlesex Turnpike, Burlington, MA 01803.
- 9. H. R. Rottmann, "Determination and Improvement of the Registration Performance of Lithographic Stepping Systems," Kodak Microelectronics Seminar Proceedings (INTERFACE '79), Eastman Kodak Company, Rochester, NY, 1979 (to be published).
- L. D. Yau, "Correlation between Process-Induced In-Plane Distortion and Wafer Bowing in Silicon," Appl. Phys. Lett. 33, 756 (1978).
- H. R. Rottmann, J. Fierro, W. Herr, and T. Sethe, "Characterization of an Internal Image Size Standard," Kodak Microelectronics Seminar Proceedings (INTERFACE '78), Publication No. G-49, Standard Book No. 0-87985-226-7, Eastman Kodak Company, Rochester, NY, 1978.
- D. Nyyssonen, "Linewidth Measurement with an Optical Microscope," Appl. Opt. 16, 2223 (1977).

Received March 12, 1979; revised January 24, 1980

The author is located at the IBM Data Systems Division laboratory, East Fishkill (Hopewell Junction), New York 12533.